Pakistan J. Zool., vol. 53(4), pp 1525-1535, 2021 DOI: https://dx.doi.org/10.17582/journal.pjz/20200420000447

The Arabian Camel, *Camelus dromedarius* Interferon Alpha: Cloning, Expression in *Escherichia coli, in vitro* Refolding and Cytotoxicity on Triple Negative Breast Cancer Cell Line MDA-MB-231

Hesham Saeed[1]*, Manal Abdel-Fattah[1], Ahmad Eldoksh[1], Farid S. Ataya[2] and Manal Shalaby[3]

[1]Department of Biotechnology, Institute of Graduate Studies and Research, Alexandria University, Alexandria, Egypt.
[2]Biochemistry Department, College of Science, Riyadh, King Saud University, Saudi Arabia.
[3]Genetic Engineering and Biotechnology Research Institute (GEBRI), City for Scientific Research and Technology Applications, New Borg Al-Arab City, Alexandria, Egypt.

Article Information
Received 20 April 2020
Revised 30 May 2020
Accepted 02 June 2020
Available online 04 June 2021

Authors' Contribution
HS supervised the experiments and prepared the manuscript. MA conducted the experiments evaluated the results. AE evaluated and validated the results. FA supervied the study and did some experiments. MS helped in manuscript revision and preparation.

Key words
***Camelus dromedaries*, Cloning, Expression, Inclusion bodies, Interferon**

ABSTRACT

The open reading frame encoding interferon alpha (IFNα) of the camel liver, *Camelus dromedarius* was isolated and cloned using reverse transcription-PCR. Sequence analysis of that gene showed a 564-bp encoding a protein of 187 amino acids with a predicted molecular weight of 21 kDa. Basic local alignment search tool (BLAST) sequence analysis revealed that *C. dromedarius* IFNα gene shares high sequence identity with IFNα genes of other species, including *C. ferus*, *Vicugna pacos*, and *Homo sapiens*. Expression of *C. dromedarius* IFNα cDNA in *Escherichia coli* revealed a fusion protein with a weight of 22.5 kDa after induction of expression with IPTG for 5 h. The recombinant IFNα was expressed in the form of inclusion bodies that were separated and solubilized *in vitro* and the protein was refolded using SDS and KCl. The folded protein is then purified using on Ni-NTA Agarose affinity chromatography and the purity was judged by SDS-PAGE. Moreover, the effect of the recombinant IFNα of the viability of cancer cell line was assessed by MTT assay. Morphological study showed that *C. dromedarius* IFNα protein inhibited cell survival of MDA-MB-231 triple negative breast cancer cells.

INTRODUCTION

The term interferon (IFN) was first coined by Alick Isaacs and Jean Lindemann in 1957 at the National Institute for Medical Research in London to describe an antiviral compound produced by virus infected chick cells that were able to interfere with viral infection (Isaacs and Lindemann, 1957). Since then, research pertaining to the discovery, characterization, and development of novel IFNs has continued for over 60 years (Meager, 2009). IFNs belong to a pleiotropic family of cytokines that play an important role in controlling cellular growth and apoptosis, and in the response to infections (Kaplan *et al*., 2017). IFNs are glycosylated proteins having molecular weight ranging from 20 to 25 kDa. They are produced in response to a variety stimuli including viral, bacterial, parasitic infections, inflammation, and tumorigenesis by various body cells like epithelia, endothelia, stroma, and cells of the immune system (Baldo, 2014; Borish and Steinke, 2003; Vacchelli *et al*., 2013; Peng *et al*., 2007). IFNs play important role in cell proliferation and differentiation, activation of immune cells, chemotaxis, inflammation, and apoptosis (Tayal and Kalra, 2008; Vacchelli *et al*., 2012). IFNs are classified-based on the receptors they interact with-into three major classes namely, type I, II, and III. Each type is encoded from different gene and has specific chromosomal localization, protein structures and biological activity (Fischer *et al*., 2018). Type II and III IFNs consist only of IFNγ and IFN while type I IFN consists of IFNα, β, δ, ε, ζ, κ ,, and ω (Klotz *et al*., 2017). The most common cytokine that has the longest record of use in clinical oncology is Type I IFNα as it is used in over 40 countries for the treatment of hematological malignancies and certain solid tumors such as melanoma, renal carcinoma, and Kaposi's sarcoma (Meager, 2009; Ferrantini *et al*., 2007). Moreover,

* Corresponding author: hsaeed1@ksu.edu.sa
0030-9923/2021/0004-1525 $ 9.00/0
Copyright 2021 Zoological Society of Pakistan

recombinant IFN-α2b is used for the treatment of recurrent melanomas (Cooksley, 2004) and IFN-α for the treatment of Hepatitis B and C, and HIV in combination with other antiviral drugs (Shepherd *et al*., 2000). Although different subtypes of IFNα essentially bind to the same receptors, they affect many biological functions and show distinct antiviral activities (Gibbert *et al*., 2013). Many interferon genes belonging to different classes have been cloned and expressed in both prokaryotic and eukaryotic hosts. Among these INFs types are from human, camel, pig, cat, horse, turkey, goose, zebra fish, and Atlantic salmon (Srikanth *et al*., 2019; Abdel-Fattah *et al*., 2019; Barathiraja *et al*., 2018; Wang *et al*., 2020; Steinbach *et al*., 2002; Suresh *et al*., 1995; Tian *et al*., 2014; Altmann *et al*., 2003; Guo *et al*., 2019; Robertsen *et al*., 2003). To the best of our knowledge, the IFNα from the Arabian one-humped camel, *Camelus dromedarius*, has not been reported yet. This camel is the most important animals in the Arabian Peninsula, for its high cultural and economic value beside the recent increasing research interest (Al-Swailem *et al*., 2010; Ataya *et al*., 2014; Malik *et al*., 2018). The aim of the present study was to clone, express, purify, and characterize IFNα found in the liver of *C. dromedarius*.

MATERIALS AND METHODS

Chemicals and reagents

Chemicals and reagents used in this study were chromatographic or molecular biology grade as appropriate. Water was either de-ionized or milli-Q-grade.

Tissue collection and total RNA isolation and purification

Liver tissue samples (1 g) from adult male *C. dromedarius* were collected immediately after scarification (The Northern Riyadh Slaughtering House, Riyadh, Saudi Arabia) submerged in 5 mL of RNA later solution (Ambion, Courtabeuf, France), and kept at 4 °C, overnight; thereafter samples were kept at -80 °C. Total RNA was isolated and purified from 100 mg of liver tissue using the RNeasy Mini Kit (Qiagen, Cat#80204, Ambion, Courtabeuf, France) with a DNase digestion step following the manufacturer's protocol. Liver tissue was homogenized in 1.0 mL of RLT lysis solution containing 1% 2-mercaptoethanol using a rotor-stator homogenizer (Medic Tools, Switzerland). The total RNA was eluted by 100 µL nuclease free water and its concentration, purity, and integrity were determined using the Agilent 2100 Bioanalyzer System and Agilent total RNA analysis kit, according to the manufacturer's protocols (Agilent Technologies, Waldbronn, Germany). Purified RNA samples with an RNA integrity number in the 7-10 range were used for first strand cDNA synthesis.

Synthesis of first strand cDNA and isolation of C. dromedarius *IFNα gene*

The first strand cDNA was synthesized from 2 micrograms of total RNA following the manufacturer's protocol of the ImProm-II Reverse Transcription System (A3800, Promega, Madison, USA). The full-length *C. dromedarius* IFNα cDNA was obtained by PCR in a final volume of 50 µL, consisting of 25 µL 2X high-fidelity master mix (GE Healthcare, USA), 3 µL (30 pmol) each of IFNα forward primer containing an *Eco*RI restriction site (5′-GAATTC ATGTCCCCAGTGGCTCGACC-3′) and reverse primer containing a *Hind*III restriction site (5′-AAGCTTTCTTTCTTGCAAGTGTCTCGC-3′), and 5 µL cDNA. Amplification was performed using the following cycling conditions; 1 cycle at 95°C for 5 min, followed by 30 cycles at 95°C for 30 s, 55°C for 30 s, and 72 °C for 1 min. A final extension step was carried out at 72°C for 5 min. The PCR products were resolved on a 1.5% agarose gel in TEA buffer, stained and visualized with 0.5 µg/mL ethidium bromide and UV light. The separated bands of the amplified gene of expected size were cut from the gel and purified using the QiAquick gel extraction kit (Qiagen, Cat # 28706, Ambion, Courtabeuf, France).

Cloning and sequencing of full-length IFNα cDNA

The plasmid cloning pGEM®-T Easy vector (Promega, Cat # A1360, Madison, USA) was used to clone the purified PCR product corresponding to IFNα cDNA to facilitate sequencing and sub-cloning into the pET28a (+) expression vector. The ligation reaction was using 4 µL of PCR product, 1 µL (50 ng) of pGEM®-T-Easy vector, 1 µL of 10X ligase buffer, and 1 U of ligase enzyme and 3µL nuclease free water to a final volume of 10 µL. Reaction tubes were incubated at 16 °C for 16 h, and 5 µL from the ligation mixure was used to transform *E. coli* JM109 competent cells, according to the previously published methods of Sambrook *et al*. (1989). Screening was carried out on selective LB/ isopropyl-β-D-1-thiogalactopyranoside (IPTG)/X-gal/ampicillin/ agar plates. Recombinant plasmids were purified from selected mostly white colonies using the PureYield Plasmid Miniprep System (Promega, Cat #A1222, Madison, USA) and the cloned insert was sequenced according to the methods of Sanger *et al*. (1977) using the T7 (5′-TAATACGACTCACTATAGGG-3′) and SP6 (5′-TATTTAGGTGACACTATAG-3′) sequencing primers. Sequence analysis was carried out using the DNAStar, BioEdit, and ClustalW programs.

Phylogenetic tree and structural modeling analysis

A phylogenetic tree was constructed according to the

methods of Dereeper *et al*. (2008), using the Phylogeny.fr software (http://www.phylogeny.fr). The nucleotide and protein sequences for *C. dromedarius* IFNα cDNA were analyzed using the basic local alignment search tool (BLAST) programs BLASTn and BLASTp (http://www.ncbi.nlm.nih.gov), respectively, and multiple sequence alignments were carried out using the ClustalW, BioEdit, DNAStar, and Jalview programs. The translated amino acid sequence from the cDNA sequence was obtained using the translation tool on the ExPasy server (http://web.expasy.org/translate/). The protein structure prediction was obtained by submitting and amino acid sequence to the Swiss-Model server, and the structural data were analyzed using the PDB viewer program. Finally, the predicted 3D structure model of IFNα was built based on multiple threading alignments using the local threading meta-server (LOMET) and iterative TASSER assembly simulation (Ortiz, *et al*., 2002; Roy *et al*., 2010).

Subcloning of IFNα gene into pET-28a (+) expression vector

The IFNα cDNA insert was liberated from the pGEM-T-Easy vector using 2 units each of *Eco*RI and *Hind*III restriction enzymes and the appropriate buffer according to the methods of Sambrook *et al*. (1989) and purified after electrophoresis from the agarose gel using the QIAquick Gel Extraction Kit (Qiagen, Cat # 28706, Ambion, Courtabeuf, France). The purified IFNα gene was ligated with pET-28a (+) expression vector cut with the same enzymes as previously described. Subsequently, 5 µL of the ligation reaction was used to transform *E. coli* BL21(DE3) pLysS (Promega, Cat. # P9801, USA) competent cells, according to the methods of Sambrook *et al*. (1989). Recombinant *E. coli* BL21(DE3) pLysS harboring the pET-28a (+) vector were screened for on selective LB/IPTG/X-gal/kanamycin/agar plates and by using the colony PCR strategy utilizing the IFNα gene-specific primers.

Expression of C. dromedarius *IFNα cDNA in E. coli BL21(DE3) pLysS*

E. coli BL21(DE3) pLysS containing the recombinant pET28a (+) plasmid were used to inoculate one liter of LB medium supplemented with 34 µg/mL kanamycin and incubated at 37°C for 4 h with shaking at 250 rpm. The induction of IFNα expression was initiated from 0.6 optical density culture at 600 nm by the addition of 1 mM IPTG and kept for 5 h incubation at 37°C under continuous shaking. The bacterial cells were harvested by centrifugation at 8000 rpm for 20 min at 4°C and the biomass was re-suspended in 10 mL of 0.1 M potassium phosphate buffer, pH 7.5, containing 50% glycerol. The bacterial cell suspension was then ultrasonicated on an ice-bath using 4 x 30-s pulses, and the clear supernatant containing the expressed protein was collected from the cell debris by centrifugation at 10,000 rpm for 10 min at 4°C.

Protein determination

Protein concentration was determined using Coomassie brilliant blue G-250 (1976), using 0.5 mg/mL of bovine serum albumin as a standard.

Sodium dodecyl sulfate gel electrophoresis (SDS-PAGE) and western blotting analysis

Expression of recombinant *C. dromedarius* IFNα in *E. coli* was evaluated by performing a 12% SDS-PAGE according to the methods of Laemmli (1970). After electrophoresis, the gel was stained with Coomassie Brilliant Blue R-250 followed by de-staining in a solution of 10% (v/v) methanol and 10% (v/v) acetic acid. Recombinant *C. dromedarius* IFNα protein was detected by western blotting using 6x-His-Tag monoclonal antibody (His. H8, Cat# MA1-21315, Thermo Fisher Scientific) at a 1:1000 dilution according to the methods of Towbin *et al*. (1979). Goat anti-mouse IgG labeled with horse radish peroxidase (Invitrogen Cat# G-21040) secondary antibody was used at a dilution of 1:2000. The membrane was developed using the chromogenic substrate 3, 3′, 5, 5′- tetramethylbenzidine liquid substrate system (Sigma-Aldrich, Cat# T0565).

Solubilization and refolding of C. dromedarius *recombinant IFNα inclusion bodies*

The inclusion bodies present in the pellets after ultrasonication were recovered by centrifugation and washed three times in 20 mM Tris-HCl, pH 8.0. Then, they were solubilized by continuous stirring on an ice-bath with denaturation buffer containing 50 mM M Tris-HCl (pH 8.0), 0.3 M NaCl, and 2% SDS until the solution became clear and the product was kept at 4°C overnight. The excess precipitated SDS was eliminated by centrifugation for 10 min at 10,000 rpm and 4°C. Subsequently, 400 mM of KCl was added to the supernatant and the solution was kept at 4°C overnight. Thereafter, the precipitate was discarded by centrifugation and the clear supernatant was dialyzed overnight against 50 mM potassium phosphate buffer (pH 7.5) and applied to a nickel affinity column (He and Ohnishi, 2017; Bornhorst and Falke, 2000).

Single step affinity purification of C. dromedarius *recombinant IFNα*

Recombinant IFNα in the solubilized inclusion bodies was purified using a single-step High-Select High Flow

nickel affinity chromatography column (1.0 cm × 1.0 cm) (Sigma-Aldrich, Cat. # H0537) previously washed with 5 bed volumes of de-ionized water, and equilibrated with 5-bed volumes of 50 mM potassium phosphate buffer (pH 7.5) containing 20 mM imidazole. A solution of solubilized inclusion bodies was applied to the column and the column was washed with 5-bed volumes of equilibration buffer. The bound recombinant IFNα was eluted with 50 mM potassium phosphate buffer (pH 7.5) containing 500 mM imidazole. The collected fractions were measured at 280 nm against blank buffer solution containing appropriate concentrations of imidazole and the fractions presented in the second peak were pooled together and dialyzed overnight against 50 mM potassium phosphate buffer (pH 7.5). The purity of the dialyzed recombinant IFNα was evaluated by performing 12% SDS-PAGE.

Cytotoxicity of recombinant C. dromedarius *IFNα on a breast cancer cell line*

Cells from the MDA-MB-231 triple negative breast cancer line, obtained from ATCC, were cultured in Dulbecco's Modified Eagle's Medium supplemented with 10% fetal bovine serum (Sigma-Aldrich Co., USA), 100 U/mL penicillin, and 100 mg/mL streptomycin, and maintained in 5% CO_2 at 37°C. An MTT assay was performed by seeding the cells in 96 well plates at a density of 15,000 cells/well and after an incubation period of 24 h, the cells were treated with varied concentrations of IFNα protein; control cells received culturing medium in phosphate buffer saline (PBS) solution. A subsequent incubation was carried out for 24 h after which, cells were washed twice with PBS followed by the addition of 3-(4,5-dimethyl-2-thiazolyl)-2,5 diphenyl-2H-tetrazolium bromide (MTT) (Serva Co.) reagent to each well at a concentration of 10 µL of 5 mg/mL in 100 µL serum free medium. Incubation was continued for 4 h at 37°C, following which the medium was discarded, 100 µL of DMSO was added to each well, the plates were shaken for 10-15 min, and the absorbance was measured at 490 nm (Abdel-Fattah *et al*., 2019).

Statistical analysis

GraphPad Prism 6.0 Software was used to perform statistical analyses. One way or two way ANOVAs (followed by Tukey or Sidak's posttest) were used where appropriate. Data are presented as the mean ± SEM or ± SD from at least two independent experiments.

RESULTS AND DISCUSSION

Nucleotide sequence analysis of C. dromedarius IFNα

To date, most information about type I IFNs has originated from studies on IFNs from other species such as human, red-crowned crane, equine, porcine, goose, salmon, turkey, and cattle (Srikanth *et al*., 2019; Tian *et al*., 2014; Steinbach *et al*., 2002; Li *et al*., 2019; Guo *et al*., 2019; Robertsen *et al*., 2003; Suresh *et al*., 1995; Barathiraja *et al*., 2018), and limited data are available about IFNs from *C. dromedarius*, the one-humped Arabian camel (Abdel-Fattah *et al*., 2019). In the present study, the full-length cDNA open reading frame of *C. dromedarius* IFNα was isolated by reverse transcription-PCR using gene specific primers designed from the available expressed sequence tag camel genome project database (http://camel.Kacst.edu.sa/). The PCR product corresponding to 561 nucleotides represents the entire open reading frame of *C. dromedarius* IFNα (Fig. 1). The purified PCR product was cloned first into the pGEM-T-Easy vector and the cDNA insert was sequenced using T7 and SP6 primers. The generated nucleotide sequence was deposited in the GenBank database under the accession number MK055340. The nucleotide sequence of the putative *C. dromedarius* IFNα gene has a statistically significant similarity score to numerous IFNα genes from other species (Table I). To determine the relatedness of *C. dromedarius* IFNα with known amino acid sequences from other species available in the GenBank database, a multiple sequence alignment was conducted (Fig. 2). The percentage identity of *C. dromedarius* IFNα with other species was 98% for *Camelus ferus* (GenBank accession # XP_014408676), 73% for *Equus asinus* (XP_014686765), 70% for *Sus scrofa* (NP_001158321), and 66% for *Homo sapiens* (NP_002166). A phylogenetic tree constructed from

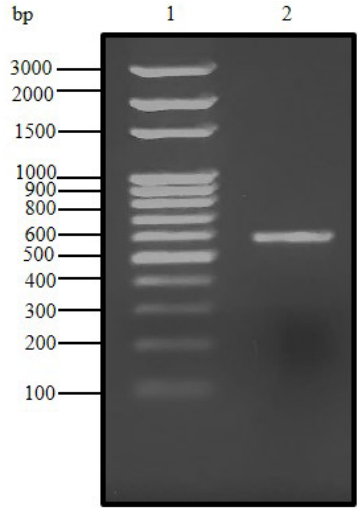

Fig. 1. Agarose gel (1.5%) electrophoresis of PCR product for *C. dromedarius* IFNα gene (Lane 2). Lane 1 represents 100 base pair DNA ladder.

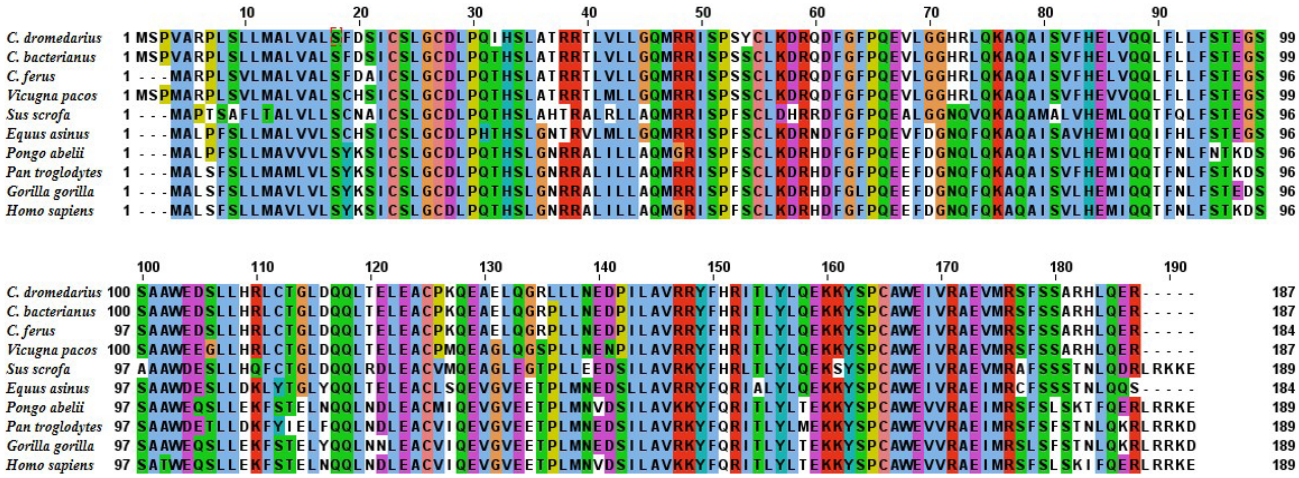

Fig. 2. Alignment of the deduced amino acid sequence of *C. dromedrius* IFNα with IFNα from other species.

the amino acid sequences of the predicted IFNα proteins deposited in GenBank indicated that *C. dromedarius* IFNα diverged along a separate evolutionary path that is distinct from other ungulates and mammalian species including human (Fig. 3).

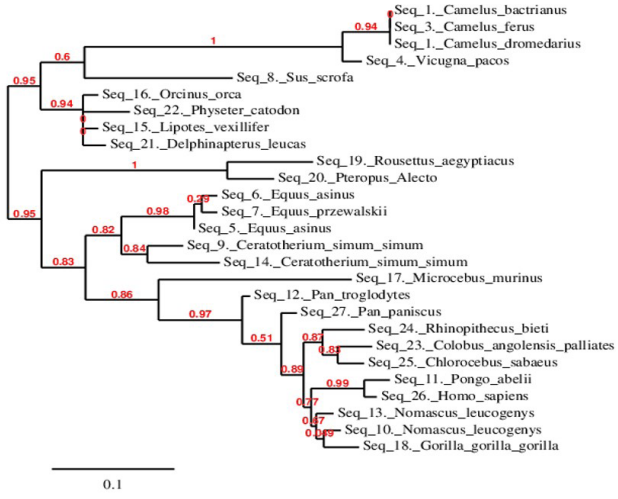

Fig. 3. Phylogenetic relationship of *C. dromedarius* IFNα and sequences from other species. Maximum likelihood tree based on complete coding sequences deposited in GenBank. Values at nodes are bootstrap ≥ 50%, obtained from 1000 re-samplings of the data.

Structural annotations and predicted 3D structure

The primary structure and protein motif secondary structural annotation for *C. dromedarius* IFNα are shown in Figures 4 and 5. The *C. dromedarius* IFNα nucleotides and deduced amino acid sequence showed an open reading frame consisting of 564 bp and 187 amino acid residues with a molecular weight of 21.339 kDa. The predicted isoelectric point was determined to be 7.67 using a computer algorithm. Analysis of secondary structural elements of *C. dromedarius* IFNα revealed the presence of some conserved

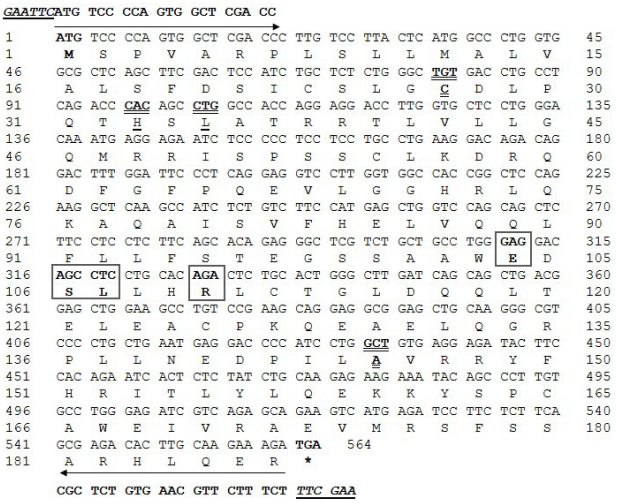

Fig. 4. Nucleotide and deduced amino acid encoding region of *C. dromedarius* IFNα. Important amino acid residues and regions include: residues that may contact N-Acetyl-2-Deoxy- are indicated by the box; residues that may contact an SO_4 ion are indicated in bold underline; residues that may contact Zn^{2+} are indicated by bold double underline, conserved amino acid residues in the IFNα protein are indicated by bold dashed underline, residues involved in IFNAR-1 binding are indicated with the circle, and residues involved in IFNAR-2 binding are indicated by the bold dashed box. Arrows indicate the location of the forward and reverse primers with restriction enzyme sites presented in bold underline italics.

Table I. Homology of the deduced amino acids of *C. dromedarius* interferon α with other species.

Animal species	Accession no.	% Identity
Camelus bacterianus	XP_010944312	100
Camelus ferus	XP_014408676	98
Vicugna pacos	XP_015098135	94
Equus asinus	XP_014686765	73
Equus przewalskii	XP_008530158	72
Sus scrofa	NP_001158321	70
Ceratotherium simum simum	XP_004436883	70
Balaenoptera acutorostrata scammoni	XP_007176876	74
Orcinus orca	XP_004275088	74
Nomascus leucogenys	XP_003260419	69
Pongo abelii	XP_002819800	68
Microcebus murinus	XP_012625263	68
Gorilla gorilla gorilla	XP_004047912	68
Rousettus aegyptiacus	XP_016015901	67
Homo sapiens	NP_002166	66

features. The first feature is the presence of 18 amino acid residues ($Q^{31, 46, 118}$, $T^{32, 114, 120}$, $R^{38, 39}$, G^{45}, W^{103}, $E^{104, 121}$, S^{106}, L^{107}, H^{109}, R^{110}, D^{117}, A^{124}) that represent the putative IFNAR-1 binding site, localized in helices A and C (Fig. 5), which is critical for receptor recognition and biological activity. The second conserved feature is the presence of a putative IFNAR-2 binding site as a part of the AB loop helix D and DE loop, which is represented by 27 amino acid residues ($L^{56,74,144,155}$, $K^{57,160, 161}$, $D^{58, 61}$, $R^{59,73,147,148,152}$, $Q^{60,66,158}$, F^{62}, G^{63}, P^{65}, $E^{67,159}$, A^{145}, H^{151}, T^{154}, E^{159}, Y^{162}, S^{163}). Analysis of glycosylation sites in *C. dromedarius* IFNα led to the prediction of one potential glycation site not occurring within the common Asn-Xaa-Ser/Thr glycation signal and this site is represented by the conserved E^{104} residue (Fig. 5). Glycosylation sites are believed to play an important role in regulating protein solubility, folding, oligomerization, and stability as well as protection against proteolytic degradation (Samudzi *et al.*, 1991). Other conserved amino acids residues involved in the binding

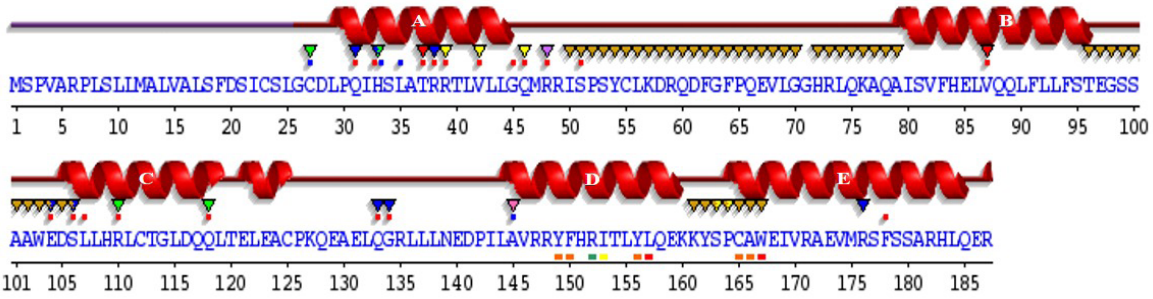

Fig. 5. Sequence annotations for *C. dromedarius* IFNα showing the location of α-helices and residues contacting ligand and ions. Secondary structure by homology (), active site residues from PDB site record (▼); residues with contact to ligand (*) and to ions (*).

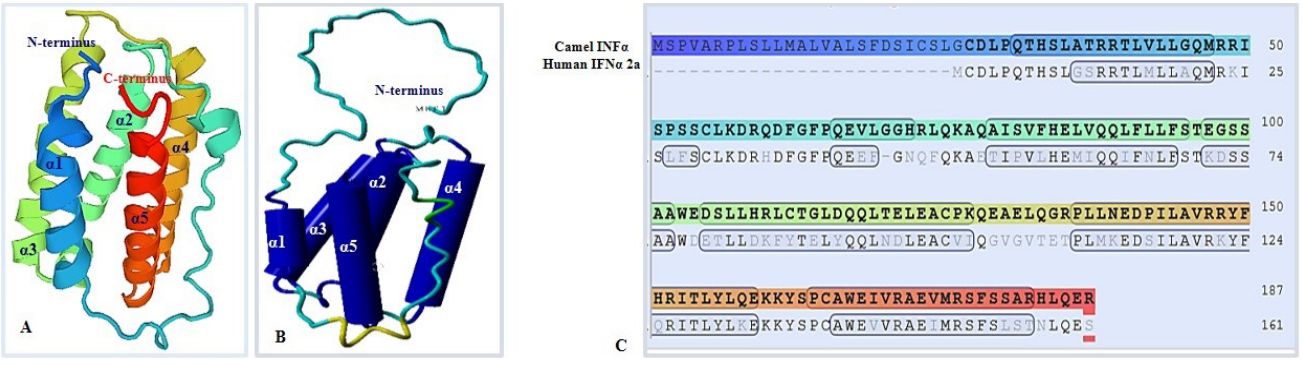

Fig. 6. Predicted 3D structure of *C. dromedarius* IFNα protein shows the overall secondary structure in ribbon form (A) and cartoon form (B). Alpha helices are labeled from α1 to α5. (C) Model-template alignment of amino acid residues of *C. dromedarius* IFNα and *Homo sapiens* IFNα2a. Components of the secondary structure are shown in blue (α helices) and brown (coils). Identical amino acid residues are shown in bold black.

of different ligands and DNA are shown in Table II. The predicted three dimensional structure of *C. dromedarius* IFNα showed that the secondary structure of the protein consisted of five alpha helices labeled from A to E as shown in Figure 6A and B. Composition of the secondary structure revealed 65.78% α-helices and 34.22% coils and turns. Analysis of the 3D structure of *C. dromedarius* IFNα revealed that the overall folding was similar to that of *H. sapiens* IFNα2a and the percent similarity and conservation in the secondary structure location was 64.6% (Fig. 6C).

Expression, solubilization, and in vitro refolding of IFNα

C. dromedarius IFNα was overexpressed in *E. coli* cells upon induction with 1 mM IPTG and appeared in insoluble inclusion bodies that were easily separated upon sonication and centrifugation at 12,000 rpm for 10 min at 4°C, leaving behind a supernatant devoid of IFNα protein as shown in Figure 7A. Western blotting analysis for recombinant *C. dromedarius* IFNα inclusion bodies protein with 6x-His-Tag monoclonal antibody revealed an immune-reacted band at 22.5 kDa (Fig. 7B and C). To recover soluble IFNα from the inclusion bodies, the SDS/KCl method was performed (Fig. 8A Lanes 3-7). Recovered, solubilized, and refolded IFNα inclusion bodies were then subjected to nickel-affinity chromatography and bound IFNα was eluted using 500 mM imidazole (Fig. 8B). The purified IFNα showed a unique single protein band at 22.5 kDa (Fig. 8C).

Cytotoxicity of C. dromedarius *IFNα on a breast cancer cell line*

IFNα has shown potential beneficial effects in various types of tumours such as hepatocellular carcinoma

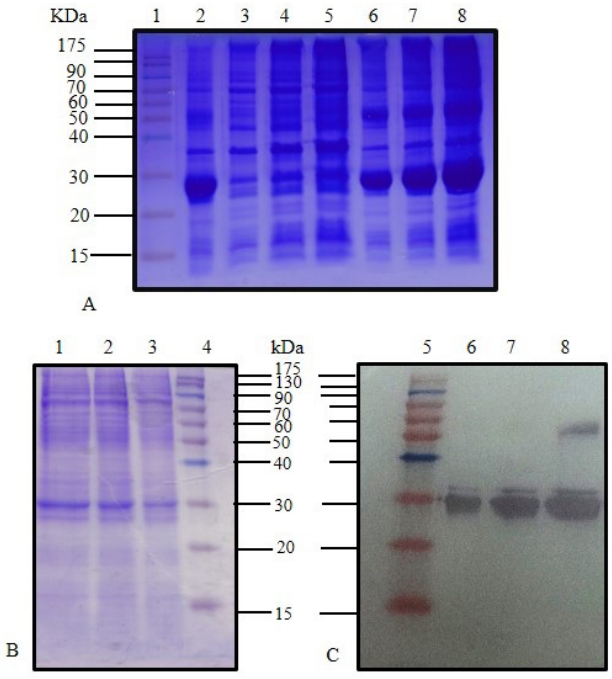

Fig. 7. SDS-PAGE (12%) for IPTG induced *E. coli* BL21(DE3) pLysS pET28 a (+) harboring *C. dromedarius* IFNα cDNA (Lane 2), IPTG induced culture supernatant (Lanes 3-5), and IPTG induced culture inclusion bodies (Lanes 6-8). (B) SDS-PAGE (12%) for IPTG induced culture (Lanes 1-3) and western blotting analysis with 6x-His-Tag monoclonal antibody (1:1000 dilution) for IPTG induced culture (Lanes 6-8). Lanes 1 (Panel A), 4 (Panel B) and 5 (Panel C) represent pre-stained molecular weight protein markers.

Table II. Conserved amino acid residues of *C. dromedarius* interferon α involved in different ligands and metal ions binding.

Annotation features	Amino acid residues
Contact(s) to ligands	
- N-Acetyl-2-Deoxy-2-Amino-Galactose	Gln^{133}, Gly^{134} Thr^{37}, Gly^{45}, Arg^{48}, Val^{87}, Gln^{118}, Phe^{178}
- 1,2-Ethanediol	
- Acetate ion	His^{33}
- 4-(2-Hydroxyethyl)-1-Piperazine ethanesulfonic acid	Arg^{48}, Ser^{51}
- Sulfate ion	Gln^{31}, Arg^{38}, Arg^{39}, Val^{42}, Gln^{46}
- Beta-D-Glucose, G6D=6-Deoxy-Alpha-D-Glucose	
Contact(s) to metals	Glu^{104}, Ser^{106}, Leu^{107}, Arg^{110}
-Nickel (ii) ion	
-Zinc ion	Cys^{27}, His^{33}
-Chloride ion	His^{33}, Ala^{145}
	His^{33}, Leu^{35}
Nucleic acids binding residues	
	Leu$^{35, 41}$, Ala$^{36, 124}$, Arg$^{38, 39}$, Val^{41}, His ^{109,183}, Thr^{113,120}, Gly^{114}, Gln^{117}, Glu$^{121, 186}$, Ser^{179}

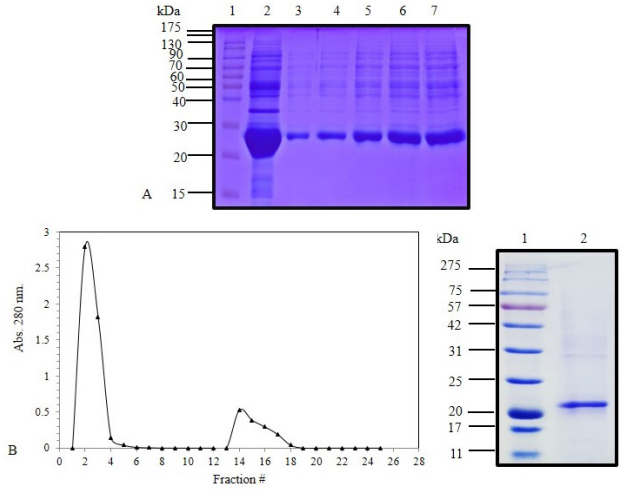

Fig. 8. (A) SDS-PAGE (12%) for IPTG induced *E. coli* BL21(DE3) pLysS pET 28 a (+) harboring IFNα cDNA inclusion bodies protein (Lane 2) and solubilized IFNα inclusion bodies (Lanes 3-7). (B) Elution profile of *C. dromedarius* IFNα after nickel affinity chromatography. Column flow rate was adjusted to be 3 mL/5 min. (C) SDS-PAGE (12%) for nickel affinity purified camel IFNα protein (Lane 2). Lanes 1 in Panel A and B represent pre-stained molecular weight protein markers.

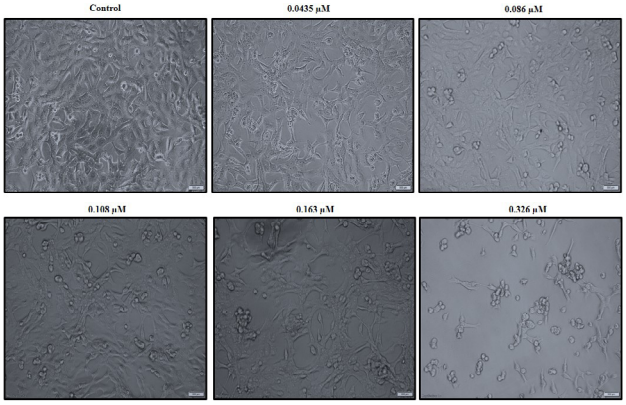

Fig. 9. *C. dromedarius* IFNα alters the morphology of the MDA-MB-231 triple negative breast cancer cell line in a dose dependent manner. Cells were treated with varied concentrations of purified recombinant *C. dromedarius* IFNα (0.0435-0.326 µM) for 24 h. Cells exhibited morphological changes indicated by shrinkage, detachment from the substratum, and rounding up as the concentration of IFNα protein increased compared with that observed for the control untreated cells (C). Magnification was 40X.

(Zhang *et al*., 2019), ovarian cancer (Green *et al*., 2016), and head and neck squamous cell carcinoma (Yang *et al*. 2019). However, the effects of recombinant *C. dromedarius* IFNα on human cancer cells have not been fully elucidated.

To study the effects of *C. dromedarius* IFNα on the MDA-MB-231 triple negative breast cancer cell line, cells were treated with varied concentrations of the purified recombinant protein and the morphology and viability of the cells were examined. The morphological changes observed after 24 h of treatment are shown in Figure 9.

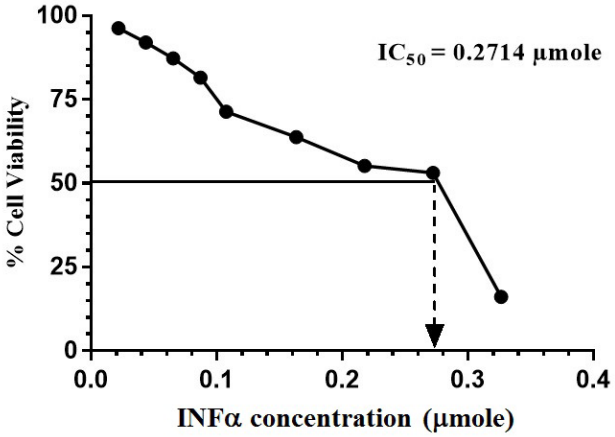

Fig. 10. MTT assay was performed and the % cell viability was calculated compared to that of the control cells. GraphPad Prism 6 was used to calculate the IC_{50} of *C. dromedarius* IFNα protein.

Cells appeared rounded up, were easily detachable, and exhibited shrinkage and reduction in size as the concentrations of the recombinant protein increased compared with that of untreated control cells (Fig. 9) suggesting inhibition of cell viability. To investigate the effect of *C. dromedarius* IFNα protein on cell viability, MTT assays were performed. The results demonstrated that IFNα inhibits the viability of cells in a dose dependent manner and the IC50 was calculated as 0.2714 µmole (Fig. 10). Type I IFNs are among the most widely used human recombinant therapeutic proteins for the treatment of several cancers and various viral infections. In addition, within the 13 alpha subtypes, only IFNα2A (Roferon A) and IFNα2b (Intron A) have been approved by the FDA and marketed for therapeutic use. Since these proteins are not glycosylated, the biopharmaceutical industry is able to use *E. coli* as a host cell factory to produce them (Ghasriani *et al*., 2013).

In conclusion, in this study, we presented cloning, expression, *in vitro* re-folding, and characterization of a novel *C. dromedarius* IFNα protein. Additionally, cytotoxicity of the recombinant protein was addressed using a triple negative breast cancer cell line; however, further research is required to unravel the role of *C. dromedarius* IFNα as a potential anti-cancer agent.

Declarations of interest

The authors declare that there is no conflict of interest for this article and there is no financial employment, consultancies, honoraria, stock ownership or options, expert testimony, grants or patents received or pending, royalties related to this manuscript. Moreover, the authors declare that this work has not been published nor simultaneously submitted for publication elsewhere. All authors agree to the submission of this manuscript.

REFERENCES

Abdel-Fattah, M., Saeed, H., El-Shennawy, L., Shalaby, M., Embaby, A., Ataya, F., Mahmoud, H. and Hussein, A., 2019. The Arabian camel, *Camelus dromedarius* interferon epsilon: Functional expression, *in vitro* refolding, purification and cytotoxicity on breast cancer cell lines. *PLoS One*, **14**: e0213880. https://doi.org/10.1371/journal.pone.0213880

Al-Swailem, A.M., Shehara, M.M., Adu-Duhier, F.M., Al-Yamani, E.J., Al-Busadah, K.A., Al-Arawi, M.S., Al-Khider, A.Y., Al-Muhaimeed, A.N., Al-Qahtani, F.H., Manee, M.M., Al-Shomrani, B.M., Al-Qhtani, S.M., Al-Harthi, A.S., Akdemir, K.C., Inan, M.S. and Otu. H.H., 2010. Sequencing, analysis and annotation of expressed sequence tags for *Camelus dromedaries*. *PLoS One*, **5**: e10720. https://doi.org/10.1371/journal.pone.0010720

Altmann, S.M., Mellon, M.T., Distel, D.L. and Kin, C.H., 2003. Molecular and functional analysis of an interferon gene from the zebrafish, *Danio rerio*. *J. Virol*., **77**: 1992–2002. https://doi.org/10.1128/JVI.77.3.1992-2002.2003

Ataya, F.S., Al-Jafari, A.A., Daoud, M.S., Al-Hazzani, A.A., Shehata, A., Saeed, H.M. and Fouad, D., 2014. Genomics, phylogeny and in Silico analysis of mitochondrial glutathione Stransferase-Kappa from the camel *Camelus dromedarius*. *Res. Vet. Sci*., **97**: 46–54. https://doi.org/10.1016/j.rvsc.2014.04.004

Baldo, B.A., 2014. Side effects of cytokines approved for therapy, *Drug Saf*., **37**: 921-943. https://doi.org/10.1007/s40264-014-0226-z

Barathiraja, S., Gangadhara, P.A.V., Umapathi, V., Dechamma, H.J. and Reddy, G.R., 2018. Expression and purification of biologically active bovine interferon λ3 (IL28B) in *Pichia pastoris*. *Protein Expr. Purif*., **145**: 14–18. https://doi.org/10.1016/j.pep.2017.12.007

Borish, L.C. and Steinke, J.W., 2003. Cytokines and chemokines. *J. Allergy clin. Immunol*., **111**: S460–S475. https://doi.org/10.1067/mai.2003.108

Bornhorst, J.A. and Falke, J.J., 2000. Purification of proteins using polyhistidine affinity tags. *Methods Enzymol*., **326**: 245–254. https://doi.org/10.1016/S0076-6879(00)26058-8

Bradford, M.M., 1976. A rapid and sensitive method for the quantitation of microgram quantities of protein utilizing the principle of protein-dye binding. *Anal. Biochem*., **72**: 248–254. https://doi.org/10.1016/0003-2697(76)90527-3

Cooksley, W.G., 2004. The role of interferon therapy in hepatitis B. *Med. Gen. Med*., **6**: 16.

Dereeper, A., Guignon, V., Blanc, G., Audic, S., Buffet, S., Chevenet, F., Dufayard, J-F., Guindon, S., Lefort, V., Lescot, M., Claverie, J-M. and Gascuel, O., 2008. Phylogeny.fr: Robust phylogenetic analysis for the non-specialist. *J. Nucl. Acids Res*., **36**: W465–W469. https://doi.org/10.1093/nar/gkn180

Ferrantini, M., Capone, I. and Belardelli, F., 2007. Interferon-α and cancer: Mechanism of action and new perspectives of clinical use. *Biochimie*, **89**: 884–893. https://doi.org/10.1016/j.biochi.2007.04.006

Fischer, C.D., Wachoski-Dark, G.L., Grant, D.M., Bramer, S.A. and Klein, C., 2018. Interferon epsilon is constitutively expressed in equine endometrium and up-regulated during the luteal phase. *Anim. Reprod. Sci*., **195**: 38–43. https://doi.org/10.1016/j.anireprosci.2018.05.003

Ghasriani, H., Belcourt, P.J., Sauvé, S., Hodgson, D.J., Brochu, D., Gilbert, M. and Aubin, Y., 2013. A single N-acetylglucosamine residue at threonine 106 modifies the dynamics and structure of Interferon α2a around the glycosylation site. *J. biol. Chem*., **288**: 247–254. https://doi.org/10.1074/jbc.M112.413252

Gibbert, K., Schlaak, J.F., Yang, D. and Dittmer, U., 2013. IFN-alpha subtypes: Distinct biological activities in anti-viral therapy. *Br. J. Pharmacol*., **168**: 1048–1058. https://doi.org/10.1111/bph.12010

Green, D.S., Nunes, A.T., Annunziata, C.M. and Zoon, K.C., 2016. Monocyte and interferon based therapy for the treatment of ovarian cancer. *Cytokine Growth Factor Rev*., **29**: 109–115. https://doi.org/10.1016/j.cytogfr.2016.02.006

Guo, Y., Xu, Y., Kang, X., Meng, C., Gu, D., Zhou, Y., Xiong, D., Geng, S., Jiao, X. and Pan, Z., 2019. Molecular cloning and functional analysis of TRAF6 from Yangzhou great white goose Anser anser. *Dev. comp. Immunol*., **101**: 103435. https://doi.org/10.1016/j.dci.2019.103435

He, C. and Ohnishi, K., 2017. Efficient renaturation

of inclusion body proteins denatured by SDS. *Biochem. biophys. Res. Commun*., **490**: 1250–1253. https://doi.org/10.1016/j.bbrc.2017.07.003

Isaacs, A. and Lindemann, J., 1957. Virus interference. I. The interferon. *Proc. R. Soc. Lond. B. Biol. Sci*., **147**: 258–267. https://doi.org/10.1098/rspb.1957.0048

Kaplan, A., Lee, M.W., Wolf, A.J., Limon, J.J., Becker, C.A., Ding, M., Murali, R., Lee, E.Y., Wong, G.C.L. and Underhill, D.M., 2017. Direct Antimicrobial Activity of IFN-β. *J. Immunol*., **198**: 4036–4045. https://doi.org/10.4049/jimmunol.1601226

Klotz, D., Baumgartner, W. and Gerhauser, I., 2017. Type I interferons in pathogenesis and treatment of canine diseases, *Vet. Immunopathol*., **191**: 80–93. https://doi.org/10.1016/j.vetimm.2017.08.006

Laemmli, U.K., 1970. Cleavage of structural proteins during the assembly of the head of bacteriophage T4. *Nature*, **227**: 680–685. https://doi.org/10.1038/227680a0

Li, S., Gong, M., Xie, Y., Shao, J., Zhao, F., Zhang, Y. and Chang, H., 2019. A novel type I interferon, interferon alphaomega shows antiviral activity against foot-and-mouth disease virus *in vitro*. *Microb. Pathog*., **127**: 79–84. https://doi.org/10.1016/j.micpath.2018.11.040

Malik, A., Khan, J.M., Alamery, S.F., Fouad, D., Labrou, N.E., Daoud, M.S., Abdelkader, M.O. and Ataya, F.S., 2018. Monomeric Camelus dromedarius GSTM1 at low pH is structurally more thermostable than its native dimeric form. *PLoS One*, **13**: e0205274. https://doi.org/10.1371/journal.pone.0205274

Meager, A., 2009. The interferons: Past, present and future, Dig. Liver Dis. 3, 3–8. Noël, N., Béatrice, B.J., Huot, N., Goujard, C., Lambotte, O., Müller-Trutwin, M., 2018. Interferon-associated therapies toward HIV control; The back and forth. *Cytok. Growth Factor Rev*., **40**: 99–112. https://doi.org/10.1016/j.cytogfr.2018.03.004

Ortiz, A.R., Strauss, C.E. and Olmea, O., 2002. MAMMOTH (Matching molecular models obtained from theory): An automated method for model comparison. *Protein Sci*., **11**: 2606–2621. https://doi.org/10.1110/ps.0215902

Peng, F.W., Duan, Z.J., Zheng, L.S., Xie, Z.P., Gao, H.C., Zhang, H., Li, W.P. and Hou, Y.D., 2007. Purification of recombinant human interferon-epsilon and oligonucleotide microarray analysis of interferon-epsilon-regulated genes. *Protein Expr. Purif*., **53**: 356–362. https://doi.org/10.1016/j.pep.2006.12.013

Robertsen, B., Bergan, V., Rokenes, T., Larsen R. and Albuquerque, A., 2003. Atlantic Salmon interferon genes: cloning, sequence analysis, expression and biological activity. *J. Interferon Cytokine Res*., **23**: 601–612. https://doi.org/10.1089/107999003322485107

Roy, A., Kucukural, A. and Zhang, Y., 2010. I-TASSER: A unified platform for automated protein structure and function prediction. *Nat. Protoc*., **5**: 725–738. https://doi.org/10.1038/nprot.2010.5

Sambrook, J., Frisch, E. and Maniatis, T., 1989. *Molecular cloning: A laboratory manual*, second ed., Cold Spring Harbor Laboratory Press, New York.

Samudzi, C.T., Burton, L.E. and Rubin, J.R., 1991. Crystal structure of recombinant rabbit interferon-gamma at 21±7 AI resolution. *J. biol. Chem*., **266**: 21791–21797. https://doi.org/10.2210/pdb1rig/pdb

Sanger, F., Nicklen, S. and Coulson, A.R., 1977. DNA sequencing with chain-terminating inhibitors. *Proc. natl. Acad. Sci. U. S. A*., **74**: 5463–5467. https://doi.org/10.1073/pnas.74.12.5463

Shepherd, J., Waugh, N. and Hewitson, P., 2000. Combination therapy (interferon alfa and ribavirin) in the treatment of chronic hepatitis C: A rapid and systematic review. *Hlth. Technol. Assess*., **4**: 1–67. https://doi.org/10.3310/hta4330

Srikanth, K., Yoganand, K.N.R., Smita, H., Ranjith Kumar, C.T., Anand, B. and Sivaprakasam, S., 2019. Novel glycosylated human interferon alpha 2b expressed in glycoengineered *Pichia pastoris* and its biological activity: N-linked glycoengineering. *Enzy. Mic. Technol*., **128**: 49–58. https://doi.org/10.1016/j.enzmictec.2019.05.007

Steinbach, F., Mauel, S. and Beier, I., 2002. Recombinant equine interferons: Expression cloning and biological activity. *Vet. Immunol. Immunopathol*., **84**: 83–95. https://doi.org/10.1016/S0165-2427(01)00396-8

Suresh, M., Karaca, K., Foster, D. and Sharma, J.M., 1995. Molecular and functional characterization of Turkey interferon. *J. Virol*., 69: 8159–8163. https://doi.org/10.1128/JVI.69.12.8159-8163.1995

Tayal, V. and Kalra, B.S., 2008. Cytokines and anti-cytokines as therapeutics an update. *Eur. J. Pharmacol*., **579**: 1–12.

Tian, L., Zhao, P., Ma, B., Guo, G., Sun, Y. and Xing, M., 2014. Cloning, expression and antiviral bioactivity of Red-crowned crane interferon-α. *Gene*, **544**: 49–55. https://doi.org/10.1016/j.gene.2014.04.036

Towbin, H., Staehelin, T. and Gordon, J., 1979. Electrophoretic transfer of proteins from

polyacrylamide gels to nitrocellulose sheets: Procedure and some applications. *Proc. natl. Acad. Sci. USA*, **76**: 4350–4354. https://doi.org/10.1073/pnas.76.9.4350

Vacchelli, E., Galluzzi, L., Eggermont, A., Galon, J., Tartour, E., Zitvogel, L. and Kroemer, G., 2012. Trial Watch: Immunostimulatory cytokines. *Oncoimmunology*, **1**: 493–506. https://doi.org/10.4161/onci.20459

Vacchelli, E., Eggermont, A., Fridman, W.H., Galon, J., Zitvogel, L., Kroemer, G., Galluzzi, L., 2013. Trial watch: Immunostimulatory cytokines. *Oncoimmunology*, **2**: E24850. https://doi.org/10.4161/onci.24850

van de Loosdrech, A.A., Nennie, E., Ossenkoppele, G.P., Beelen, R.H.J. and Langenhuijsen, M.A.C., 1991. Cell mediated cytotoxicity against U937 cells by human monocytes and macrophages in a modified colorimetric MTT assay: A methodological study. *J. Immunol. Met.*, **141**: 15–22. https://doi.org/10.1016/0022-1759(91)90205-T

Wang, X., Li F., Han, M., Jia, S., Wang, L., Qiao, X., Jiang, Y., Cui, W., Tang, L., Li, Y. and Xu, Y.G., 2020. Cloning, prokaryotic soluble expression, and analysis of antiviral activity of two novel feline IFN-ω proteins. *Viruses*, **12**: pii: E335. https://doi.org/10.3390/v12030335

Yang, W., Jiang, C., Xia, W., Ju, H., Jin, S., Liu, S., Zhang, L., Ren, G., Ma, H., Ruan, M. and Hu, J., 2019. Blocking autophagy flux promotes interferon-alpha-mediated apoptosis in head and neck squamous cell carcinoma. *Cancer Lett.*, **451**: 34–47. https://doi.org/10.1016/j.canlet.2019.02.052

Zhang, Y., Li, X., Zhang, Y., Wang, L., Xu, J., Du, J. and Guan, Y., 2019. Pegylated interferon α inhibits the proliferation of hepatocellular carcinoma cells by down regulating miR-155. *Annls Hepatol.*, **18**: 494–500. https://doi.org/10.1016/j.aohep.2018.11.007